Available online at www.sciencedirect.com
SCIENCE DIRECT
Thermochimica Acta 436 (2005) 78–82
thermochimica acta
www.elsevier.com/locate/tca

Limitation of the Johnson–Mehl–Avrami (JMA) formula for kinetic analysis of the crystallization of a chalcogenide glass

A.A. Joraid *

Physics Department, Science College, Taibah University, P.O. Box 3668, Madinah, Saudi Arabia

Received 20 May 2005; received in revised form 12 July 2005; accepted 13 July 2005

Abstract

The crystallization kinetics of $Sb_{9.1}Te_{20.1}Se_{70.8}$ chalcogenide glass have been studied by differential scanning calorimetry (DSC). The effective activation energy of crystallization has been evaluated on the basis of the Kissinger equation and the method of Matusita et al. The Sestak–Berggren model has been used for the description of DSC crystallization data as it provides the best fit to the experimental results. It has been found that the Johnson–Mehl–Avrami model could be applied at very high rates of heating.

Keywords: DSC; Crystallization kinetics; Heating rate; Chalcogenide glasses; Thermal properties

1. Introduction

Chalcogenide glasses have been investigated extensively because these materials have important technological applications, such as switching, memory, and electrophotography [1]. Differential scanning calorimetry (DSC) and differential thermal analysis (DTA) are the thermal methods most commonly applied to studying the behavior of glass crystallization [2–4].

The heat flow, ϕ, evolved during crystal growth, can be expressed by the following kinetic equation [5,6]:

$$\phi = \Delta H \frac{\mathrm{d}\chi}{\mathrm{d}t}, \tag{1}$$

where ΔH is the heat of crystallization. The crystallization fraction χ can be expressed as a function of time according to the Johnson–Mehl–Avrami (JMA) transformation equation [7,8]:

$$\chi(t) = 1 - \exp[-(Kt)^n], \tag{2}$$

K is defined here as the effective overall reaction rate constant, which reflects both the rate of nucleation frequency and the crystal growth rate, n, the Avrami exponent, is a numerical factor depending on the nucleation and growth processes. The constant K usually has an Arrhenian temperature dependence:

$$K = K_0 \exp\left(-\frac{E_c}{RT}\right), \tag{3}$$

where K_0 is the frequency factor and E_c is the effective activation energy.

Eqs. (2) and (3) provide the basis for nearly all the experimental treatments in DSC. The isothermal transformation rate $\mathrm{d}\chi(t)/\mathrm{d}t$ can be given from Eq. (2) as

$$\frac{\mathrm{d}\chi}{\mathrm{d}t} = nK(1-\chi)[-\ln(1-\chi)]^{1-1/n}. \tag{4}$$

So, the heat flow can be given as

$$\phi = \Delta H n K(1-\chi)[-\ln(1-\chi)]^{1-1/n}. \tag{5}$$

In cases when JMA equation (5) is not valid, the empirical Sestak–Berggren (SB) model [9,10] should be used for the description of the crystallization kinetics of some chalcogenide glasses:

$$\phi = \Delta H K \chi^m (1-\chi)^n, \tag{6}$$

* Tel.: +966 48226462; fax: +966 48233727.
E-mail addresses: aaljoraid@kaau.edu.sa, ajoraid@health.net.sa.

0040-6031/$ – see front matter © 2005 Elsevier B.V. All rights reserved.
doi:10.1016/j.tca.2005.07.005

where m is an integer that depends on the dimensionality of the crystal.

It is possible to compute the activation energy using some known methods. Matusita et al. [11] have suggested a method specifically for non-isothermal experiments. The volume fraction of crystallites χ precipitated in a glass heated at constant heat rate α is related to the activation energy for crystallization E_c as

$$\ln[-\ln(1-\chi)] = -n\ln\alpha - 1.052\frac{mE_c}{RT} + \text{constant}. \quad (7)$$

If the crystallization fraction χ is determined at a fixed temperature but at different heating rates, the Avrami exponent n can be obtained from the slope of the following equation:

$$\left.\frac{\mathrm{d}\{\ln[-\ln(1-\chi)]\}}{\mathrm{d}(\ln\alpha)}\right|_T = -n. \quad (8)$$

In fact, it is known that the double-logarithmic function in Eq. (7) may be linear even when the JMA model is not adequate. The limits of applicability of the JMA equation are well known, but Malek [12–15] has proposed a simpler method to test the applicability of the JMA model. The test is based on Eqs. (5) and (6) and on the $y(\chi)$ and $z(\chi)$ functions. Under non-isothermal conditions these functions are given by

$$y(\chi) = \phi\ \exp\left(\frac{E_c}{RT}\right), \quad (9)$$

$$z(\chi) = \phi T^2. \quad (10)$$

These functions exhibit their maxima at χ_M and χ_P^∞, respectively, which allows one to determine the kinetics from the diagram obtained.

The kinetic exponent, m, was calculated by the relation [10,13]:

$$m = \frac{n\chi_M}{1-\chi_M}. \quad (11)$$

The aim of this study was to calculate the kinetic parameters from DSC data by a non-isothermal method and to determine the best kinetic model that describes the crystallization process of $Sb_{9.1}Te_{20.1}Se_{70.8}$ chalcogenide glass.

2. Experimental

The DSC experiments presented in this paper were preformed by using a Shimadzu DSC-60 instrument on samples encapsulated in standard aluminum sample pans in an atmosphere of dry nitrogen. To minimize the temperature gradients, the samples were will granulated to form uniform fine powder and spread as thinly as possible on the bottom of the sample pan, and the weight of sample was kept very low 2.4–3 mg. Non-isothermal DSC curves were obtained with selected heating rates 2–80 K min^{-1}. Temperature and enthalpy calibration were checked with indium (T_m = 1.56.6 °C, ΔH_m = 28.55 J g^{-1}) as standard material supplied by Shimadzu.

The $Sb_{9.1}Te_{20.1}Se_{70.8}$ chalcogenide glass was prepared using the melt–quench technique from pure elements (99.999%) in an evacuated quartz glass ampoule by melting and homogenization at 950 K for a period of 24 h. The amorphous nature and purity of the prepared material was checked by scanning electron microscope (SEM)-EDX using a Shimadzu Superscan SSX-550 apparatus.

3. Results and discussion

According to Eq. (7), the plot of $\ln[-\ln(1-\chi)]$ against $1/T$ should give a straight line, and mE_c should be obtainable from the slope of the lines for all heating rates. For $Sb_{9.1}Te_{20.1}Se_{70.8}$, the plot of $\ln[-\ln(1-\chi)]$ against $10^3/T$ is shown in Fig. 1. The resulted straight lines have slopes that decrease gradually from a low heating rate toward a high heating rate. Some deviation from linearity at high temperatures or in the region of large crystallized fractions was attributed to the saturation of nucleation sites in the final stages of crystallization.

Eq. (8) indicates that at any fixed temperature the values of the crystallization mechanism or Avrami exponent n can be obtained from the slope of the resulting lines.

The calculated values of n were not integers and showed a variation of $2.4 \le n \le 4$: this means that the crystalliza-

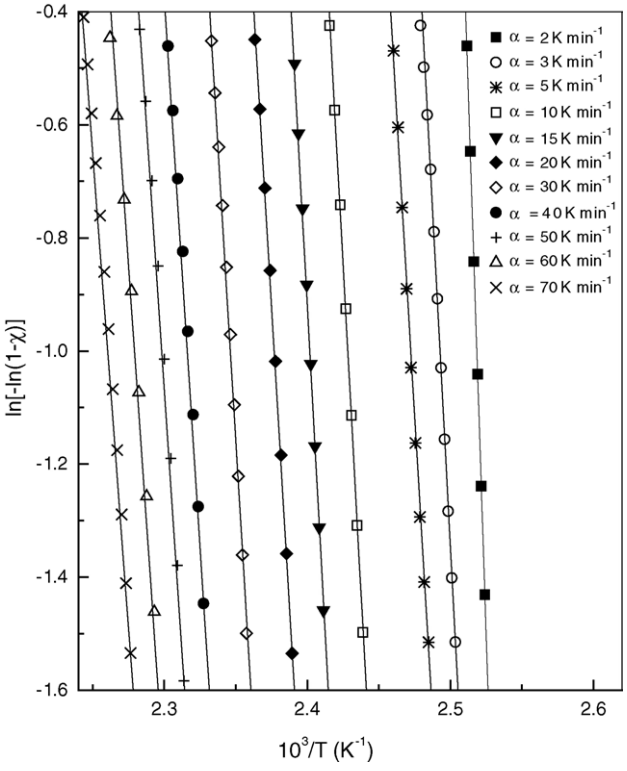

Fig. 1. The plot of $\ln[-\ln(1-\chi)]$ against $10^3/T$ for all heating rates.

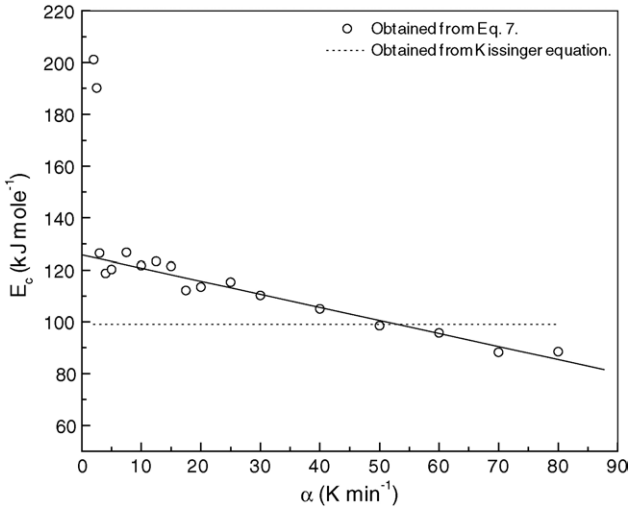

Fig. 2. The activation energy for crystallization E_c obtained by two methods. The first two experimental points at $\alpha = 2$, 2.5 K min^{-1} were excluded from curve fitting due to their anomalous values.

tion occurs by more than one mechanism [16]. These values of n may be accounted for by the possibility of a combination of two- and three-dimensional crystal growth with heterogeneous nucleation at $n - 2.4$, the possibility of three-dimensional crystal growth with heterogeneous and homogeneous nucleation at about $n \sim 2.4$, and the possibility of two-dimensional crystal growth with homogeneous nucleation at a high heating rate with $n \sim 2.4$ [16].

The activation energy for crystallization obtained for $Sb_{9.1}Te_{20.1}Se_{70.8}$ from these measurements was calculated and its variation with heating rate is shown in Fig. 2. The dotted line in Fig. 2 corresponds to the value determined by the Kissinger method:

$$\frac{\mathrm{d}[\ln(\alpha/T_P^2)]}{\mathrm{d}(1/T_P)} = -\frac{E_c}{R}.$$

Figs. 3 and 4 show the functions $y(\chi)$ and $z(\chi)$ for $Sb_{9.1}Te_{20.1}Se_{70.8}$ chalcogenide glass at different heating rates. From the analysis of these curves the maxima of $y(\chi)$ and $z(\chi)$ can be found.

The maximum of the function $z(\chi)$, χ_P^∞, is a constant and its value of $\chi_P^\infty = 0.632$ is a characteristic 'fingerprint' of the JMA model [13]. The maximum of the $z(\chi)$ function as obtained from Fig. 3 is $\chi_P^\infty \cong 0.442$, which is evidence that the mechanism of crystallization of $Sb_{9.1}Te_{20.1}Se_{70.8}$ glass does not follow the JMA.

There are small but noticeable differences among the curves for different heating rates, which can probably be attributed to thermal inertia phenomena due to lower imperfect thermal contact between the coarse-powdered sample and the bottom of the aluminum capsule [6,13,15]. The maximum value of the $y(\chi)$ function, χ_M, is always lower than the value of χ_P^∞ [13]. Fig. 4 shows a maximum value of $y(\chi)$ at $\chi_M \cong 0.393$; from this maximum the values of the kinetic exponent m can be estimated as described by Eq. (11).

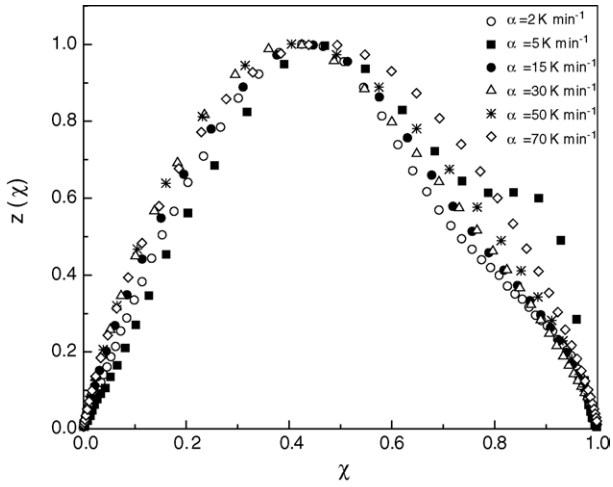

Fig. 3. Normalized $z(\chi)$ function obtained from DSC data from the non-isothermal method at different heating rates.

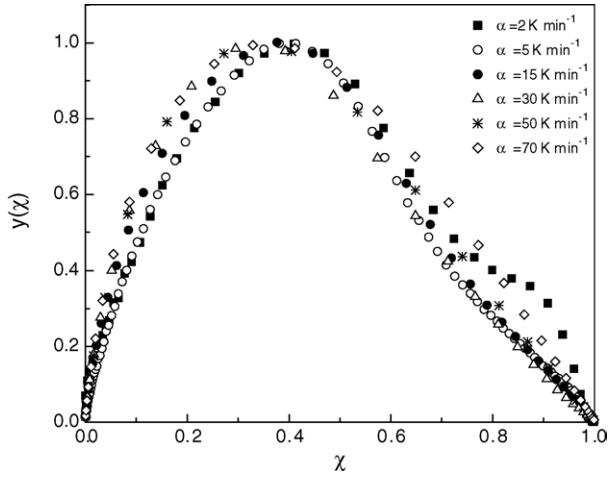

Fig. 4. Normalized $y(\chi)$ function obtained from DSC data from the non-isothermal method at different heating rates.

Theoretical DSC curves for the JMA and SB models can be calculated using Eqs. (5) and (6). For each heating rate the value of activation energy E_c was calculated, and the value of the heat of crystallization ΔH was obtained from the DSC instrument. The results are shown in Table 1.

Comparisons of the experimental data and calculated curves using the JMA and SB models are shown in Figs. 5–10 for different heating rates.

Table 1
Kinetic parameters from the JMA and SB theoretical models

α (K min^{-1})	ΔH (J g^{-1})	n	χ_M	χ_P^∞	E_c (kJ mol^{-1})
2	46.65	2.4	0.405	0.468	201.2 ± 1.3
5	55.3	2.5	0.397	0.443	120.2 ± 1.01
15	55.5	3.48	0.382	0.443	121.4 ± 1.24
30	64.9	3.87	0.339	0.413	110.2 ± 2.6
50	98.1	2.95	0.341	0.421	98.5 ± 2.7
70	63.8	2.53	0.346	0.469	88.2 ± 1.76

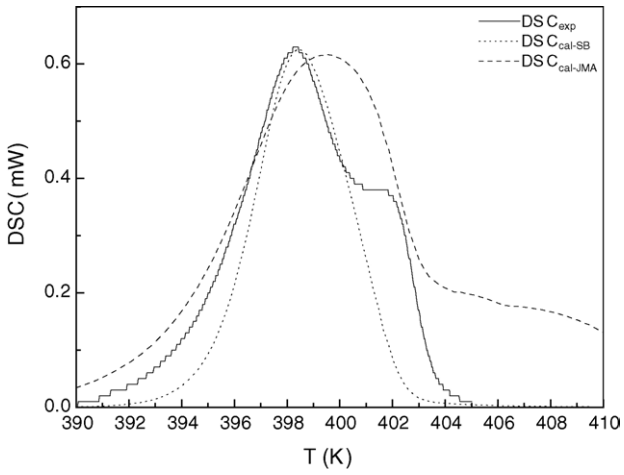

Fig. 5. Comparison of the experimental data (DSC_{exp}) and calculated curves (DSC_{cal}) using the SB and JMA models at a heating rate of 2 K min^{-1}.

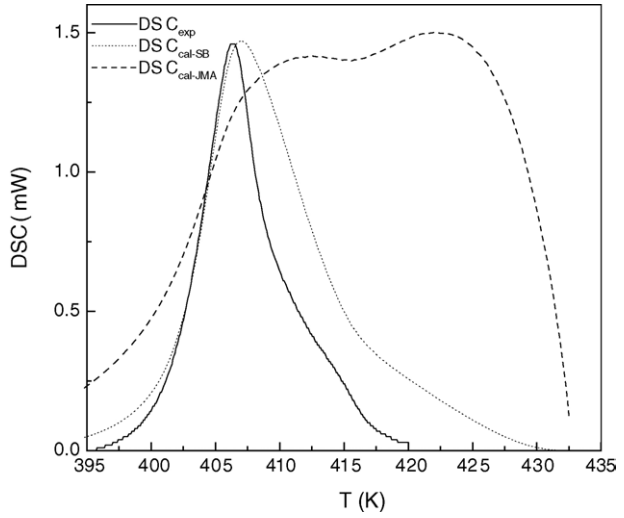

Fig. 6. Comparison of the experimental data (DSC_{exp}) and calculated curves (DSC_{cal}) using the SB and JMA models at a heating rate of 5 K min^{-1}.

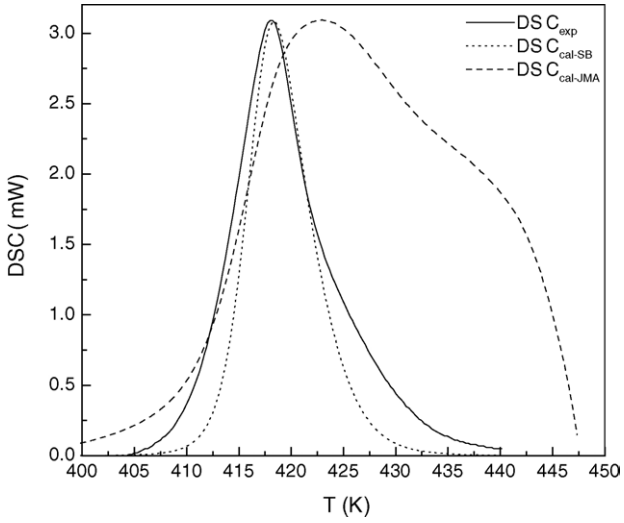

Fig. 7. Comparison of the experimental data (DSC_{exp}) and calculated curves (DSC_{cal}) using the SB and JMA models at a heating rate of 15 K min^{-1}.

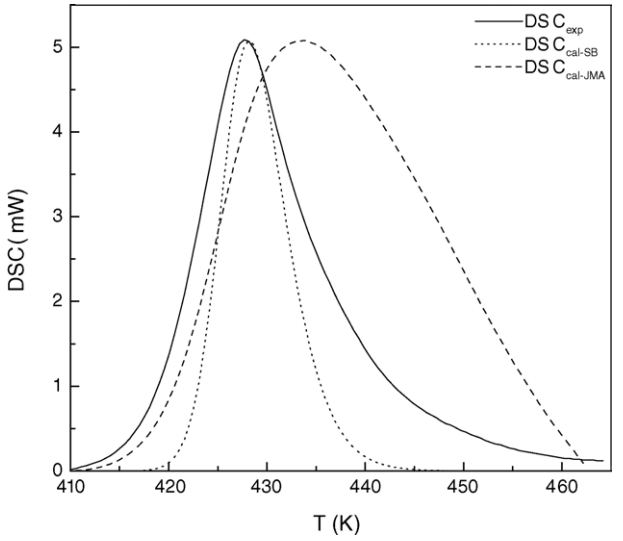

Fig. 8. Comparison of the experimental data (DSC_{exp}) and calculated curves (DSC_{cal}) using the SB and JMA models at a heating rate of 30 K min^{-1}.

A complicated shape of DSC peaks were revealed for low heating rate (2 and 3 K min^{-1}) as shown in Fig. 5. Two noticeable crystallization peaks were clearly observed.

The experimental curves show relatively good agreement with the SB model, in particular at lower heating rates. At high heating rates, $\alpha > 60$ K min^{-1}, the experimental curves are in fairly good agreement with the JMA model. Henderson [17,18] has shown that the validity of the JMA equation can be extended in non-isothermal conditions if the entire nucleation process takes place during the early stages of the transformation, and it become negligible afterward. This so-called site saturation is an important condition for the crystallization process where the crystallization rate is defined only by temperature and does not depend on the previous thermal history. It seems from the results obtained at high heating rates that the crystallization rate is too fast also, which

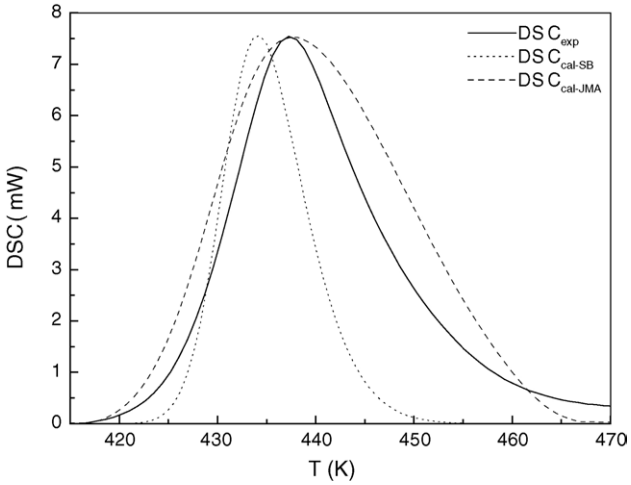

Fig. 9. Comparison of the experimental data (DSC_{exp}) and calculated curves (DSC_{cal}) using the SB and JMA models at a heating rate of 50 K min^{-1}.

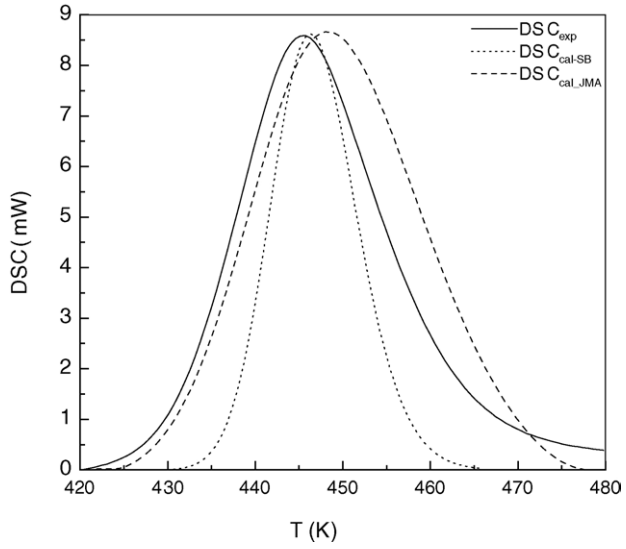

Fig. 10. Comparison of the experimental data (DSC_{exp}) and calculated curves (DSC_{cal}) using the SB and JMA models at a heating rate of 70 K min^{-1}.

makes the entire nucleation to take place during early stages of transformation. So, the situation of the validity of JMA model in non-isothermal conditions is reasonably satisfied for $Sb_{9.1}Te_{20.1}Se_{70.8}$, but only at high heating rates.

4. Conclusion

The effective activation energy for crystallization of $Sb_{9.1}Te_{20.1}Se_{70.8}$ has been determined using the Kissinger equation; a value of approximately 99 ± 4.3 kJ mol^{-1} was found. The method of Matusita et al. [11] has been used to find the kinetic parameter n, which was found to be dependent on heating rate. From non-isothermal data the maxima of the $y(\chi)$ and $z(\chi)$ functions were calculated, which allowed us to obtain the kinetic parameter m and to find an adequate model to fit the experimental results. From the results presented, the SB kinetic model was shown to be the best model to describe the crystallization process for $Sb_{9.1}Te_{20.1}Se_{70.8}$ glass. The JMA model shows some agreement with the experimental results at high heating rates.

References

[1] S.A. Khan, M. Zulfequar, M. Husain, J. Phys. Chem. Solids 63 (2002) 1787.
[2] H. Yannon, D.R. Uhlmann, J. Non-Cryst. Solids 54 (1983) 253.
[3] P.L. López, J. Vázqez, P. Villares, R. Jiménez-Garay, J. Non-Cryst. Solids 287 (2001) 203.
[4] A.A. Abu-Sehly, Physica B 325 (2003) 372.
[5] J. Sestak, W.W. Wendtlandt, Thermophysical Properties of Solids: Their Measurement and Theoretical Thermal Analysis, Elsevier, Amsterdam, 1984.
[6] E. Cernoskova, Z.G. Ivanova, V. Pamukchieva, Thermochim. Acta 316 (1998) 97.
[7] P.L. López-Almany, J. Vázqez, P. Villares, R. Jiménez-Garay, Mater. Chem. Phys. 65 (2000) 150.
[8] J. Vazquez, R. Gonzalez-Palma, P. Villares, R. Jimenez-Garay, Physica B 336 (2003) 297.
[9] J. Sestak, G. Berggren, Thermochim. Acta 3 (1971) 1.
[10] D.V. Silva, C.A. Ribeiro, M.S. Crespi, J. Therm. Anal. Calorim. 72 (2003) 151.
[11] K. Matusita, T. Komatsu, R. Yokota, J. Mater. Sci. 19 (1984) 291.
[12] J. Malek, J. Therm. Anal. Calorim. 56 (1999) 763.
[13] J. Malek, Thermochim. Acta 355 (2000) 239.
[14] J. Malek, J. Mater. Res. 16 (2001) 7.
[15] J. Shanelova, J. Malek, M.D. Alcala, J.M. Criado, J. Non-Cryst. Solids 351 (2005) 557.
[16] N. Ziani, M. Belhadji, L. Heireche, Z. Bouchaour, M. Belbachir, Physica B 358 (2005) 132.
[17] D.W. Henderson, J. Therm. Anal. 15 (1979) 325.
[18] D.W. Henderson, J. Non-Cryst. Solids 30 (1979) 301.